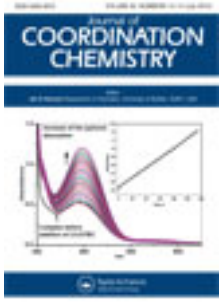

Journal of Coordination Chemistry
Publication details, including instructions for authors and subscription information:
http://www.tandfonline.com/loi/gcoo20

Synthesis, crystal structure, and spectroscopic properties of a new Zn(II) coordination polymer with 4-(2-picolinylhydrazide) methylene benzoic acid containing the $(H_2O)_8(CH_3OH)_2$ cluster

Shi-Liang Chen [a], Zheng Liu [a], Jin-Hong Xia [b] & Yan-Hong Li [c d]

[a] College of Chemical and Biological Engineering, Guilin University of Technology, Guilin 541004, P.R. China

[b] College of Electronic Engineering, Guilin University of Electronic Technology, Guilin 541004, P.R. China

[c] Guangxi Key Laboratory of Environmental Engineering, Protection and Assessment, Guilin 541004, P.R. China

[d] College of Environmental Science and Engineering, Guilin University of Technology, Guilin 541004, P.R. China

Accepted author version posted online: 04 May 2012.Published online: 22 May 2012.

To cite this article: Shi-Liang Chen, Zheng Liu, Jin-Hong Xia & Yan-Hong Li (2012) Synthesis, crystal structure, and spectroscopic properties of a new Zn(II) coordination polymer with 4-(2-picolinylhydrazide) methylene benzoic acid containing the $(H_2O)_8(CH_3OH)_2$ cluster, Journal of Coordination Chemistry, 65:13, 2234-2246, DOI: 10.1080/00958972.2012.690866

To link to this article: http://dx.doi.org/10.1080/00958972.2012.690866

Journal of Coordination Chemistry
Vol. 65, No. 13, 10 July 2012, 2234–2246

Synthesis, crystal structure, and spectroscopic properties of a new Zn(II) coordination polymer with 4-(2-picolinylhydrazide) methylene benzoic acid containing the $(H_2O)_8(CH_3OH)_2$ cluster

SHI-LIANG CHEN†, ZHENG LIU*†, JIN-HONG XIA‡ and YAN-HONG LI§¶

†College of Chemical and Biological Engineering, Guilin University of Technology, Guilin 541004, P.R. China
‡College of Electronic Engineering, Guilin University of Electronic Technology, Guilin 541004, P.R. China
§Guangxi Key Laboratory of Environmental Engineering, Protection and Assessment, Guilin 541004, P.R. China
¶College of Environmental Science and Engineering, Guilin University of Technology, Guilin 541004, P.R. China

(*Received 19 November 2011; in final form 28 March 2012*)

A zinc coordination polymer, $\{[ZnL(H_2O)_2]\cdot 2(H_2O)(CH_3OH)\}_n$ (**1**) (H_2L = 4-(2-picolinylhydrazide) methylene benzoic acid), consisting of a trapeziform chain was synthesized and characterized by elemental analysis, UV, IR, and single-crystal X-ray diffraction. Single-crystal structure of this compound reveals that the coordination geometry of zinc is a slightly distorted trigonal bipyramid and the trapeziform chains are further assembled into a 3-D network *via* hydrogen-bonding and π–π interactions. A water–methanol cluster, $(H_2O)_8(CH_3OH)_2$, is observed in this complex. The electronic absorption spectrum was attributed to intra-ligand electronic transitions. The spectrum of **1** indicates strong fluorescence at λ_{ex} = 282 nm in the fluorescence spectrum at room temperature; the fluorescence gradually quenches with rising temperature. With increasing scan rate, the reversible redox process of Zn^{2+}/Zn^{+} changes into a quasi-reversible one.

Keywords: Zinc complex; Crystal structure; Water cluster; Fluorescence spectrum; Electrochemical analyses

1. Introduction

Zinc is a necessary trace element in biological systems and plays a very important role in life science. Organozinc carboxylate derivatives have antitumor, antiviral, antifungal antibacterial, anti-inflammatory activity, and rich structural chemistry [1–3]. They are widely used in ion exchange, catalysts, gas storage, absorption, fluorescence relay, and construction of intriguing supramolecular structures [4–7]. The presence of nitrogen and oxygen donors makes these compounds effective and stereospecific catalysts for

*Corresponding author. Email: lisa4.6@163.com; piaocsl@163.com

ISSN 0095-8972 print/ISSN 1029-0389 online
http://dx.doi.org/10.1080/00958972.2012.690866

oxidation, reduction hydrolysis, and may also show biological activities and other transformations of organic and inorganic chemistry [8, 9]. Some drugs have more activity as metal complexes [10, 11]. Metal complexes bridged by organic ligands are often adopted to construct coordination polymers, which can be further assembled by hydrogen-bonding, π–π interaction, or other intermolecular contacts into extended networks with higher dimensionality [12–14]. Polycarboxylates as bridges are good choices to assemble metal ions into diverse structural motifs [15–17].

We now report the syntheses of 4-(2-picolinylhydrazide) methylene benzoic acid (H_2L) and its Zn(II) coordination polymer $\{[ZnL(H_2O)_2]\cdot 2(H_2O)(CH_3OH)\}_n$ (**1**) characterized by crystal structures, infrared (IR), UV-Vis and fluorescence spectra and electrochemical properties. Single-crystal X-ray analysis reveals that the trapeziform chain structural motifs of the complex are assembled into a 3-D network *via* hydrogen-bonding and π–π interactions. The stability of the supramolecular conglomeration has a contribution of $(H_2O)_8(CH_3OH)_2$ clusters with a novel configuration.

2. Experimental

2.1. *Materials and physical measurements*

All reagents were commercially available and used without purification. Elemental analyses (C, H, and N) were performed on a Vario ELIII elemental instrument. UV-Vis absorption spectra were obtained in DMSO using a GBC UV-Vis spectrophotometer. IR spectra were recorded from 4000 cm^{-1} to 400 cm^{-1} with KBr pellets on a Shimadzu FTIR-8400 spectrophotometer. Cyclic voltammetry was measured on a CHI860D electrochemical analysis system (China) with a three-electrode system consisting of a glassy carbon (GC) electrode ($U = 3$ mm) as a working electrode, a saturated calomel electrode as a reference electrode, and a platinum wire as an auxiliary electrode. Emission/excitation spectra were carried out on a Hitachi RF-5301 fluorescence spectrophotometer.

2.2. *Synthesis of 2-picolinylhydrazide*

2-Picolinylhydrazide was obtained by reaction of 2-picolinic acid methyl ester with hydrazine hydrate (scheme 1) according to the literature [18]. Its m.p.: 98–100°C agrees with corresponding data in the literature.

2.3. *Synthesis of H_2L*

As shown in scheme 1, a solution of 2-picolinylhydrazide (0.69 g, 5 mmol) in methanol (10 mL) was added dropwise to a methanol (20 mL) solution of 4-formylbenzoic acid (0.75 g, 5 mmol) with stirring at room temperature. The resulting mixture was refluxed and stirred for 4 h at 70°C until a white precipitate formed. The precipitate was collected by filtration, washed with methanol, and desiccated in a loft drier. Anal. Calcd for $C_{14}H_{11}N_3O_3$(%): C, 62.45; H, 4.12; N, 15.61. Found: C, 62.39; H, 4.07; N, 15.73.

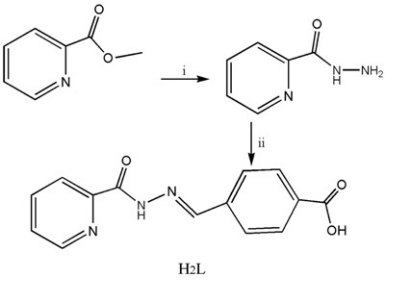

Scheme 1. i: 80% $NH_2NH_2 \cdot H_2O$, 10 h refluxing; ii: 4-formylbenzoic acid, CH_3OH, 3 h refluxing.

2.4. *Synthesis of* $\{[ZnL(H_2O)_2] \cdot 2(H_2O)(CH_3OH)\}_n$ *(1)*

$Zn(CH_3COO)_2$ hydrate (0.11 g, 0.5 mmol) in methanol (5 mL) was slowly added to a methanol solution (25 mL) of triethylamine (0.5 mL) and H_2L (0.15 g, 0.5 mmol) with stirring at 70°C. The mixture was refluxed and stirred for 2 h until a yellowish precipitate formed. The yellowish turbid solution was filtered and the filtrate slowly evaporated at room temperature resulting in yellow single crystals suitable for X-ray diffraction. Anal. Calcd for $C_{15}H_{21}N_3O_8Zn$ (%): C, 41.25; H, 4.85; N, 9.62. Found: C, 41.34; H, 4.21; N, 9.66.

2.5. *X-ray crystal structure determination*

A block single crystal with dimensions $0.19 \times 0.16 \times 0.15\,mm^3$ was mounted on a goniometer and data collection was performed on a Bruker APEX-II CCD diffractometer by the φ and ω scan technique using graphite-monochromated Mo-Kα radiation ($\lambda = 0.71073$ Å) at 296(2) K. The intensity symmetries indicate a monoclinic $P2_1/c$ space group. A total of 13,341 reflections (3217 unique) were performed within θ range 2.63–25.50°. SHELXS-97, SHELXL-97, and SHELXTL [19] were used for structure determination and refinement. The structures were solved by direct methods and all non-hydrogen atoms were obtained from the difference Fourier map and subjected to anisotropic refinement by full-matrix least-squares on F^2. All hydrogen atoms of **1** were added geometrically or positioned by difference Fourier synthesis and refined isotropically. Details concerning crystal data and refinement are given in table 1.

3. Results and discussion

3.1. *Crystal structure*

X-ray structural determination of **1** confirms the structural assignments based on spectroscopic data. Compound **1** crystallizes in $P2_1/c$ space group and consists of a 3-D polymeric structure of $\{[ZnL(H_2O)_2] \cdot 2(H_2O)(CH_3OH)\}_n$ where the zincs are connected by two discrete water molecules and one L^{2-}. The fundamental unit is

Table 1. Crystal data and structure refinements for **1**.

CCDC reference no.	825719
Empirical formula	$C_{15}H_{21}N_3O_8Zn$
Formula weight	436.72
Temperature (K)	296(2)
Wavelength (Å)	0.71073
Crystal system	Monoclinic
Space group	$P2_1/c$
Unit cell dimensions (Å, °)	
a	7.2068(8)
b	21.877(3)
c	11.1010(13)
α	90.00
β	99.178(2)
γ	90.00
Volume (Å^3), Z	1727.8(3), 4
Calculated density (Mg m^{-3})	1.679
Absorption coefficient (mm^{-1})	1.473
$F(000)$	904
Crystal size (mm^3)	$0.19 \times 0.16 \times 0.15$
θ range for data collection (°)	2.63–25.50
Limiting indices	$-8 \le h \le 8$; $-26 \le k \le 26$; $-13 \le l \le 13$
Reflections collected	13,341
Independent reflections	3217 [R(int) = 0.0393]
Refinement method	Full-matrix least-squares on F^2
Data/restraints/parameters	3217/6/231
Goodness-of-fit on F^2	0.933
Final R indices [$I > 2\sigma(I)$]	$R_1 = 0.0491$, $wR_2 = 0.1333$
R indices (all data)	$R_1 = 0.0697$, $wR_2 = 0.1489$
Largest difference peak and hole (e Å^{-3})	0.592 and −0.718

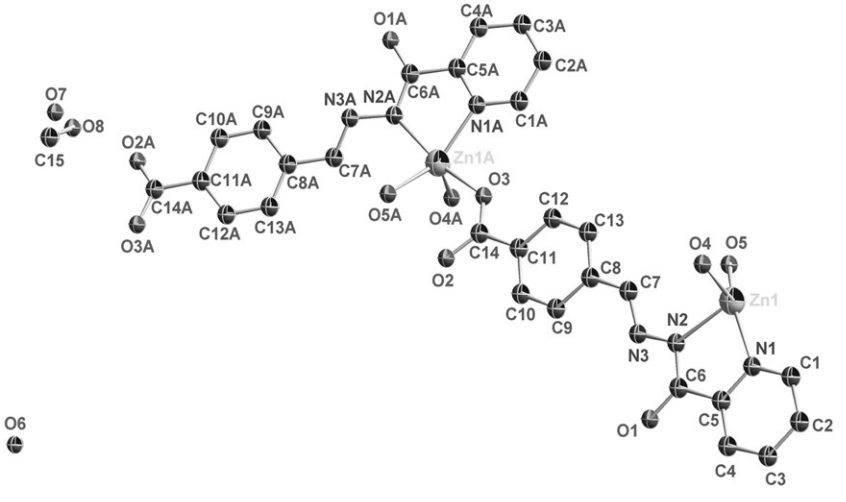

Figure 1. Molecular structure of **1**. The hydrogen atoms were omitted.
Symmetry code: A: $-x+1$, $y+1/2$, $-z+3/2$.

shown in figure 1, in which displacement ellipsoids are drawn at the 30% probability level. Selected bonds, lengths, and angles are listed in table 2.

The crystal structure shows that this complex contains crystalline water molecules and methanols. There is one crystallographically unique Zn in the crystal unit of **1**.

Table 2. Selected bond lengths (Å) and angles (°) for **1**.

N(1)–Zn(1)	2.082(5)	O(4)–Zn(1)	2.018(5)
N(2)–Zn(1)	2.099(5)	O(5)–Zn(1)	2.045(4)
O(3)–Zn(1)#1	2.054(4)	Zn(1)–O(3)#2	2.055(4)
N(2)–N(3)	1.397(6)	C(6)–O(1)	1.255(7)
C(14)–O(3)	1.246(8)	C(6)–N(2)	1.322(7)
C(14)–O(2)	1.244(9)	C(7)–N(3)	1.270(7)
C(10)–C(11)	1.398(9)	C(1)–N(1)	1.346(8)
C(11)–C(14)	1.514(8)	C(5)–N(1)	1.338(8)
C(5)–C(6)	1.505(8)		
N(1)–Zn(1)–N(2)	78.81(18)	O(3)#2–Zn(1)–N(2)	164.48(19)
O(3)#2–Zn(1)–N(1)	90.34(19)	O(4)–Zn(1)–N(1)	107.5(2)
O(4)–Zn(1)–N(2)	98.37(18)	O(5)–Zn(1)–N(1)	141.3(2)
O(5)–Zn(1)–N(2)	92.23(18)	C(14)–O(3)–Zn(1)#1	128.7(4)
O(4)–Zn(1)–O(3)#2	95.44(19)	C(6)–N(2)–Zn(1)	115.5(4)
O(5)–Zn(1)–O(3)#2	89.38(18)	N(3)–N(2)–Zn(1)	131.9(4)
O(4)–Zn(1)–O(5)	111.0(2)	C(1)–N(1)–Zn(1)	127.4(5)
C(5)–N(1)–Zn(1)	114.4(4)	C(6)–N(2)–N(3)	112.3(5)
C(7)–N(3)–N(2)	116.3(5)	O(3)–C(14)–O(2)	125.3(6)
N(1)–C(5)–C(6)	116.5(5)	O(3)–C(14)–C(11)	116.9(6)
O(1)–C(6)–C(5)	118.4(5)	O(2)–C(14)–C(11)	117.8(6)
N(2)–C(6)–C(5)	114.7(5)	N(3)–C(7)–C(8)	121.1(5)

Symmetry codes: #1: $-x+1$, $y+1/2$, $-z+3/2$; #2: $-x+1$, $y-1/2$, $-z+3/2$.

Each L^{2-} provides two nitrogen atoms from pyridine ring and C–N, respectively, to coordinate with Zn(II) forming a five-membered chelate ring of $ZnNC_2N$. The geometry of Zn(1) is a slightly distorted trigonal bipyramid with two nitrogen atoms from L^{2-}, one O from another carboxyl of L^{2-}, and two water molecules. In the ZnN_2O_3 slightly distorted trigonal bipyramid, N(1), O(4), and O(5) are located in the equatorial plane (plane equation: $-1.273x+19.177y-4.592z=-5.1928$), the distance is 0.0445 Å between Zn(1) and the plane, while O(3)A and N(2) occupy axial positions.

The Zn–N distances of 2.082(5)–2.099(5) Å fall in the reported range of 1.970(2)–2.105(2) Å in $[Zn_2(pzdc)(im)_3]_n$ [20]. The Zn–O bond lengths of 2.018(5)–2.055(4) Å are very close to those of $[Zn_2(pzdc)(im)_3]_n$ [20]. Bond angles O(4)–Zn(1)–N(1), O(5)–Zn(1)–N(1), and O(4)–Zn(1)–O(5) are 107.5(2)°, 141.3(2)°, and 111.0(2)°, respectively. The sum of these angles of 359.8° is close to 360° suggesting planar N(1), O(4), O(5), and Zn(1). The coordination geometry of Zn(1) is a slightly distorted trigonal bipyramid with a τ-value of 0.39 (the structure index is defined as $\tau=(\beta-\alpha)/60$, where α and β are the largest coordination angles, $\beta=$ O(3)#2–Zn(1)–N(2) 164.48° and $\alpha=$ O(5)–Zn(1)–N(1) 141.3°; symmetry code: #2 $-x+1$, $y-1/2$, $-z+3/2$). This type of slightly distorted trigonal bipyramid was also observed in the reported Cu(II) complex [21]. The N(1)–Zn(1)–N(2) angle of 78.81(18)° (in the chelate ring) is less than 90° and the O(5)–Zn(1)–N(2) angle of 92.23(18)° (in the inter-ring) is larger than 90°, perhaps due to the constraint of the chelating ligand. These values are 1° greater than those in hexahedral zinc complexes [20, 22] showing that the ring flexibility resulting from rotatable single bonds makes this ligand more adjustable to different geometrical requirements. The chelate ring adopts an approximately planar conformation and the observed torsion angles (table 3) (the torsion angles of C(6)–N(2)–Zn(1)–N(1), N(1)–C(5)–C(6)–N(2), and C(5)–C(6)–N(2)–Zn(1) are 0.1(4)°, −2.6(8)°, and 1.2(6)°,

Table 3. Selected torsion angles (°) and hydrogen bonds.

C(1)–N(1)–Zn(1)–N(2)	−178.1(5)	O(2)–C(14)–O(3)–Zn(1)#1	2.6(12)
C(6)–N(2)–Zn(1)–O(4)	−106.1(4)	C(11)–C(14)–O(3)–Zn(1)#1	−176.1(4)
N(3)–N(2)–Zn(1)–O(4)	80.3(5)	C(5)–N(1)–Zn(1)–O(4)	93.8(4)
C(6)–N(2)–Zn(1)–O(5)	142.2(4)	C(1)–N(1)–Zn(1)–O(4)	−82.7(5)
N(3)–N(2)–Zn(1)–O(5)	−31.3(5)	C(5)–N(1)–Zn(1)–O(5)	−81.0(5)
C(6)–N(2)–Zn(1)–O(3)#2	46.5(9)	C(1)–N(1)–Zn(1)–O(5)	102.5(6)
N(3)–N(2)–Zn(1)–O(3)#2	−127.0(7)	C(5)–N(1)–Zn(1)–O(3)#2	−170.4(4)
C(6)–N(2)–Zn(1)–N(1)	0.1(4)	N(1)–C(5)–C(6)–N(2)	−2.6(8)
N(3)–N(2)–Zn(1)–N(1)	−173.4(5)	C(5)–N(1)–Zn(1)–N(2)	−1.6(4)
Zn(1)–N(2)–N(3)–C(7)	−18.2(7)	C(8)–C(7)–N(3)–N(2)	178.4(5)
C(5)–C(6)–N(2)–Zn(1)	1.2(6)	O(1)–C(6)–N(2)–N(3)	−4.6(8)
C(6)–N(2)–N(3)–C(7)	168.1(5)	C(5)–C(6)–N(2)–N(3)	176.0(5)
C(6)–C(5)–N(1)–Zn(1)	2.7(6)	N(1)–C(5)–C(6)–O(1)	178.0(5)
C(2)–C(1)–N(1)–Zn(1)	176.8(5)	O(1)–C(6)–N(2)–Zn(1)	−179.5(5)

D–H···A	*d*(D–H)	*d*(H···A)	*d*(D···A)	∠(DHA)
O(5)–H(3 W)···O(2)#2	0.83	1.90	2.661(7)	151.0
O(5)–H(4 W)···N(3)#3	0.83	2.06	2.861(7)	161.3
O(5)–H(4 W)···O(1)#3	0.83	2.58	3.169(7)	128.8
O(4)–H(1 W)···O(1)#4	0.84	1.88	2.703(6)	168.2
O(4)–H(2 W)···O(8)#5	0.83	1.91	2.704(16)	158.1
O(6)–H(6 W)···O(6)#6	0.83	2.32	2.76(2)	114.1
O(6)–H(5 W)···O(1)#7	0.86	1.98	2.706(9)	141.0

Symmetry codes: #1: $-x+1$, $y+1/2$, $-z+3/2$; #2: $-x+1$, $y-1/2$, $-z+3/2$; #3: $-x+1$, $-y$, $-z+1$; #4: $-x$, $-y$, $-z+1$; #5: x, $y-1$, z; #6: $-x$, $-y+2$, $-z$; #7: x, $y+1$, z.

respectively) are close to the ideal 0° pattern owing to the intra-molecular conjugate. L^{2-} is non-planar with an inclination angle between pyridine from 2-picolinylhydrazide and phenyl from 4-formylbenzoic acid of 2.5°. The carboxyl of L^{2-} is monodentate with the carbonyl coordinating to Zn(II) [23].

The lattice water clusters $(H_2O)_4$ assemble by hydrogen-bonding in **1**. As shown in figures 2 and 3, the angles of each $(H_2O)_4$ cluster motifs of O5a–O7b–O5c, O7b–O5c–O7d, O5c–O7d–O5a, and O7d–O5a–O7b are 154.5°, 25.5°, 154.5°, and 25.5° (symmetry codes: a: $-x+1$, $y+1/2$, $-z+3/2$; b: $-x+1$, $y-1/2$, $-z+3/2$; c: x, $-y+1/2$, $z-1/2$; d: x, $-y+3/2$, $z-1/2$), respectively. Adding up these angles gives 360.0°, which indicates a planar structure of four oxygen atoms (O5a, O7b, O5c, and O7d). The O5a–O7d–O7b and O5c–O7b–O7d angles have the same value of 39.8°, resulting in a parallel quadrilateral consisting of two triangles with four oxygen atoms at the vertices. As shown in figure 3, the $(H_2O)_8(CH_3OH)_2$ cluster originates from $(H_2O)_4$ linking two methanols in a centrosymmetric tablet chair mode. The most interesting feature of the crystal structure is the intermolecular hydrogen-bonding and π–π stacking interaction (the centroid distances are 3.5725 Å and 3.6366 Å) (figure 4). The intermolecular hydrogen bonds (as shown in table 3) between water and L^{2-} (the distances of O···O are in the range 2.661(7)–3.169(7) Å, range of O–H···O angles, 114.1–168.2°. The separation of O(5)–H(4 W)···N(3)#3 is 2.861(7) Å (symmetry codes: #3 $-x+1$, $-y$, $-z+1$) and the angle is 161.3°) fall into the normal range of hydrogen-bonding interactions [24]. Water clusters, providing insight into the structure and characteristics of liquid water or ice [25], have been extensively studied both theoretically and experimentally due to their unusual properties and importance in many physical, chemical, and biological processes [26]. The water cluster in **1** is particularly interesting.

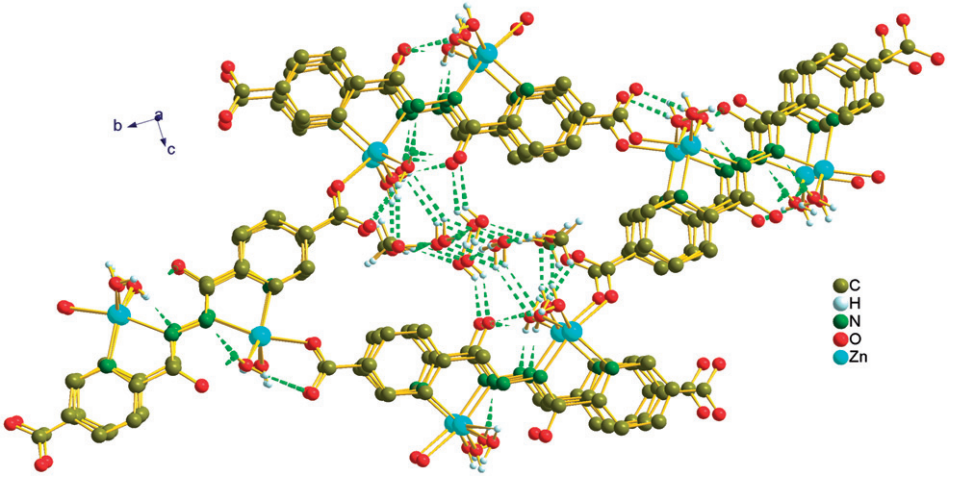

Figure 2. Perspective of the crystal packing and $(H_2O)_8(CH_3OH)_2$ clusters in the unit cell along the *a*-axis for **1**. Dashed lines indicate hydrogen bonds. Some of the hydrogen atoms were omitted for clarity.

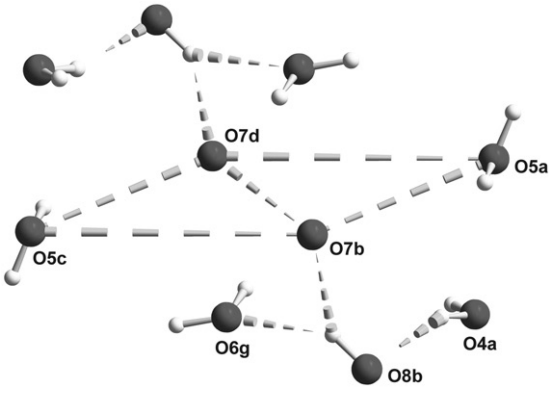

Figure 3. Detailed view of $(H_2O)_8(CH_3OH)_2$ trapped through hydrogen-bonding in **1**. Dashed lines indicate hydrogen bonds.
Symmetry codes: a: $-x+1, y+1/2, -z+3/2$; b: $-x+1, y-1/2, -z+3/2$; c: $x, -y+1/2, z-1/2$; d: $x, -y+3/2, z-1/2$; e: $-x+1, y-1/2, -z+1/2$.

A series of configurations of water clusters such as book, boat, and chair with cyclic conformation [24], as well as ring [27–30], tape [31, 32], folded-chain [33–35], helical chains [36], hanging-ladder [37], cage [38], column [39], water–methanol intermix clusters [40], and prism polyhedral structures have been reported [41–43]. However, to the best of our knowledge, such a chair-type water cluster consisting of triangles or parallel quadrilateral has not been reported.

In **1**, the polymer backbone is along the crystallographic *b*-axis. The 1-D chains are consecutively linked by O(3)–Zn(1)#1 bridges (figure 5 L) to produce a ladder coordination polymer (figure 5 T). The metal–metal distances across each polymer backbone are 11.6711(17) Å, which are longer than those in $[Zn(ip)(im)_2]_n \cdot 3nH_2O$ (the metal–metal distances of 10.391(14) Å) [44]. The 2-D layers stack in an ABABAB

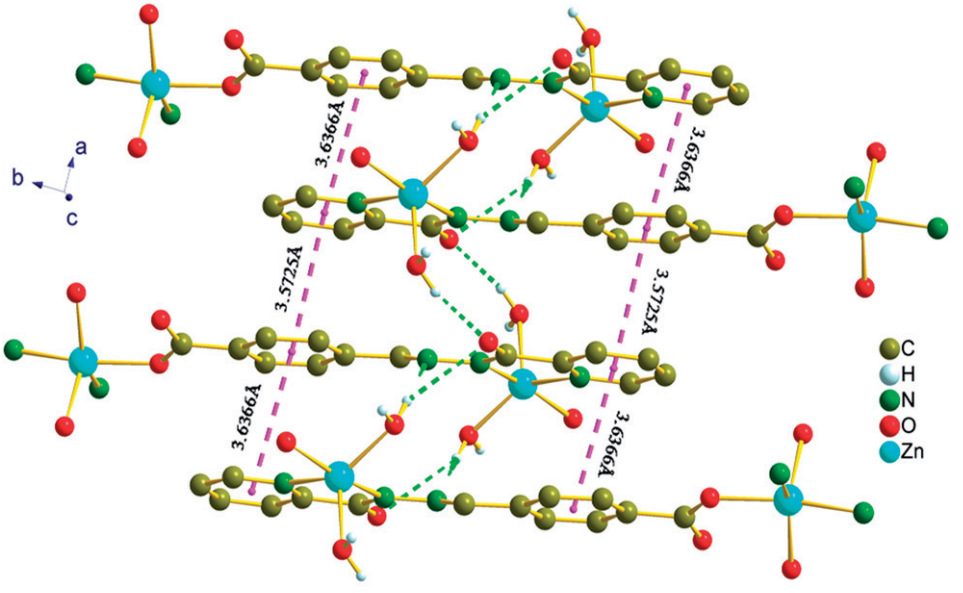

Figure 4. 2-D layer of **1** *via* hydrogen-bond interactions and face-to-face π–π stacking interactions. Some of the hydrogen atoms were omitted for clarity.

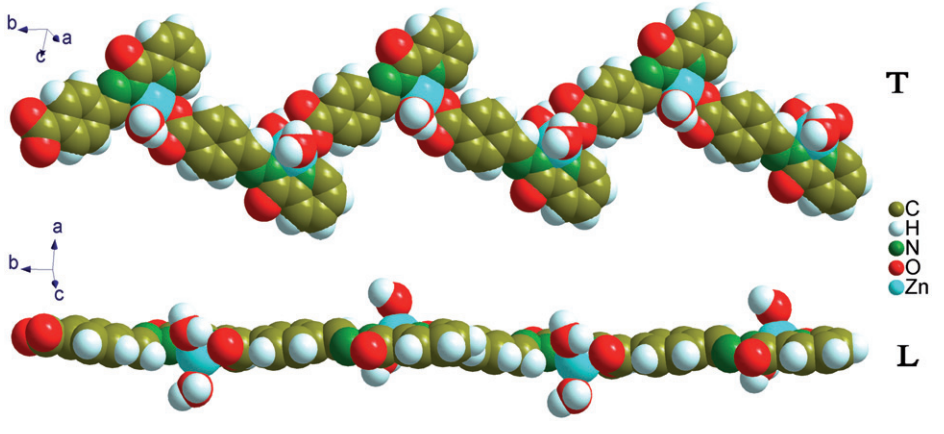

Figure 5. Perspectives of (T) 3-D ladder and (L) 1-D chain.

sequence of the ladder coordination polymer. There are water clusters and π–π stacking interactions between the 2-D layers (figure 4), forming a complicated 3-D supramolecular network. These extensive weak intermolecular interactions make an important contribution to the stability of the coordination compound.

3.2. *UV-Vis spectroscopy*

Electronic absorption spectra of the free ligand and **1** were measured in DMSO solution. UV-Vis spectrum of **1** was recorded with 5.0×10^{-5} mol L^{-1} sample.

The ligand shows two bands at 327 nm and 370 nm in the ultraviolet region assigned to a conjugated B absorption band of π-bond from benzene and an n–π^* transition of conjugation between lone-pair electron of p orbital of nitrogen in C = N [45]. The peaks at 291 and 314 nm are attributed to π–π^* and n–π^* transitions of C=N of the complex, respectively. The π–π^* transition of benzene usually appears at 245 nm [46]. The absorption spectrum of **1** displays reduced oscillator strengths and blue shifts compared with the ligand, related to the molecular structure of the complex, i.e. the planar geometry of the ligand is hampered by steric hindrance of the complex [47]. The lack of conjugation is consistent with changes observed in intensity and energy of the electronic spectra. The shift of the characteristic band indicates the formation of **1** [48].

3.3. *IR spectrum analysis*

The characteristic IR spectra of L^{2-} and **1** are presented in "Supplementary material." The IR spectrum of **1** shows significant differences from the free ligand. The absence of bands of methanamide ν(N–H) and ν(O–H) from the carboxyl in the complex suggests that deprotonated N–H and O–H coordinate with zinc [49, 50]. The absorption bands of the ligand at 1280 cm^{-1} for ν(C–N) shift to 1262 cm^{-1} in the complex indicating formation of metal–ligand bonds. Other evidence that the nitrogen of methanamide is involved in coordination is the ν(N–N) shifts 39 cm^{-1} from free ligand to complex. The difference of $\Delta\nu(\nu_{as}(COO^-)$–$\nu_{sym}(COO^-))$ is often used to determine the bonding of carboxylate complexes [51] with $\Delta\nu$ less than 200 cm^{-1}, indicating bidentate carboxylate, while larger than 200 cm^{-1} means monodentate carboxylate [52]. The $\nu_{as}(COO^-)$ and $\nu_{sym}(COO^-)$ vibrations are 1617 cm^{-1} and 1385 cm^{-1} for **1** and the difference $\Delta\nu(\nu_{as}(COO^-)$–$\nu_{sym}(COO^-))$ between these frequencies is close to those found in monodentate carboxylate (232 cm^{-1}). This observation is consistent with X-ray structural analyses. The Zn–N stretching vibration at 517 cm^{-1} is in agreement with that of a related complex [53]. The stretching frequency of O–H bonds of the water cluster is observed as a wide weak multiple absorption at 3429 cm^{-1}. The IR spectrum of ice shows the O–H stretch at 3220 cm^{-1} while that in liquid water appears at 3490 cm^{-1} and 3280 cm^{-1} [54–57]. Thus the O–H stretch in the water cluster of **1** is similar to that of liquid water.

3.4. *Fluorescence spectrum*

Photoluminescence of **1** was measured with 5.0×10^{-5} mol L^{-1} DMSO solution at room temperature. The photoluminescence spectrum of **1** is depicted in figure 6, where an intense emission at 338 nm ($\lambda_{ex} = 282$ nm) is exhibited. As a d^{10} ion, Zn(II) does not contribute to the electronic transition of the complex, which reconciles with the UV-Vis analysis. The fluorescence properties at different temperatures were determined (figure 7), showing that the fluorescence efficiency of **1** is influenced by temperature change from 25°C to 65°C with increment of 5°C. The spectra show larger fluorescence intensity of 235.209 a.u. at 25°C. Fluorescence intensity gradually lowers with increasing temperature, reaching 206.672 a.u. at 65°C. The increasing temperature may increase fluorescence quenching.

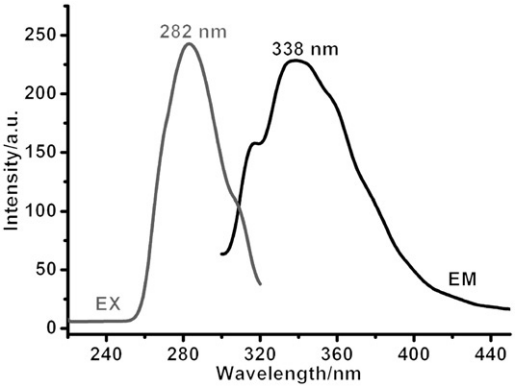

Figure 6. Excitation and emission spectra of **1**.

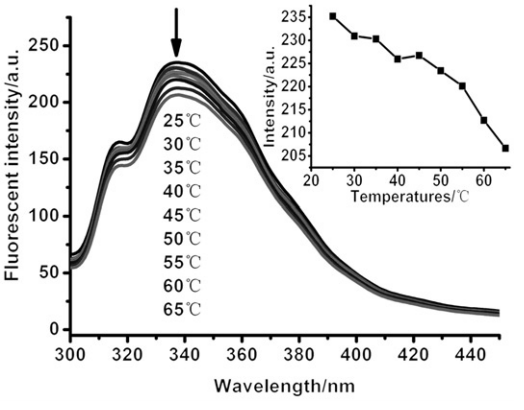

Figure 7. Fluorescence emission spectra of **1** at different temperatures and fluorescent intensity with the change in the temperature on the top right.

3.5. *Electrochemistry character*

"Supplementary material" depicts the cyclic voltammogram of **1** in DMSO containing 0.05 mol L^{-1} tetrabutylammonium bromide at different scan rates. The electrochemical data of **1** at different scan rates are listed in table 4, where the anodic and cathodic peaks correspond to Zn^{2+}/Zn^{+} [58]. The separation of the cathodic peaks of −0.529 V and anodic peak of −0.460 V (ΔE is 0.069 V) indicates that the electrochemical behavior of **1** on the GC electrode is electrochemically reversible. Values of oxidation and reduction peaks are more positive than those of $\{[Zn(ip)(Eim)_2]\cdot H_2O\}$ ($E_{pa} = -1.161$ V, $E_{pc} = -1.345$ V, $\Delta E = 0.184$ V) and $Zn(ip)(Mim)_2$ ($E_{pa} = -1.141$ V, $E_{pc} = -1.282$ V, $\Delta E = 0.141$ V) [59]. The cathodic peaks E_{pc} gradually become more negative and the cathodic peak currents (I_{pc}) increase with increasing scan rate, while the anodic peaks E_{pa} shift to more positive and anodic peak currents (I_{pa}) increase with increasing scan rate. These changes result in increasing ΔE separations and the transformation of the redox process from a reversible process to a quasi-reversible one.

Table 4. Electrochemical data at different scan rates.

Scan rate ($V\,s^{-1}$)	Cathodic peaks		Anodic peaks		Separation ΔE (V)
	E_{pc} (V)	I_{pc} (μA)	E_{pa} (V)	I_{pa} (μA)	
0.005	−0.529	2.979	−0.460	2.308	0.069
0.01	−0.532	3.955	−0.460	3.146	0.072
0.03	−0.543	6.160	−0.478	4.837	0.065
0.06	−0.547	8.134	−0.452	5.785	0.095
0.09	−0.556	9.803	−0.450	7.285	0.106
0.12	−0.560	11.280	−0.451	8.623	0.109
0.15	−0.566	12.830	−0.450	9.843	0.116
0.18	−0.575	13.300	−0.449	9.990	0.126
0.21	−0.576	13.460	−0.445	9.435	0.131
0.24	−0.578	13.480	−0.435	10.200	0.143
0.30	−0.582	13.520	−0.433	9.339	0.149
0.40	−0.597	14.050	−0.435	10.530	0.162

$\Delta E = E_{pa} - E_{pc}$.

This suggests that donor such as unsaturated oxygen and nitrogen of a ligand can stabilize a low oxidation state, such as Zn^{+}, more than a saturated one, by π-back bonding between metal and oxygen and nitrogen [60].

4. Conclusion

A metal coordination polymer, $\{[ZnL(H_2O)_2]\cdot 2(H_2O)(CH_3OH)\}_n$, has been synthesized and characterized. Crystal structure shows that there is one ligand and one crystallographically unique Zn in the symmetrical unit. Zn(1) with a slightly distorted trigonal bipyramid geometry is coordinated by two nitrogen atoms of L^{2-} and three oxygen atoms of another L^{2-} and two water molecules. The trapeziform chains are further assembled into a 3-D metal–organic framework *via* water clusters through hydrogen-bonding and π–π interaction. The electronic absorption spectra are attributed to intra-ligand electronic transitions. Experimental fluorescence measurements show that the complex emits strong fluorescence at $\lambda_{ex} = 282$ nm and rising temperature leads to fluorescence quenching. With increasing scan rate, the redox process gradually changes to quasi-reversible.

Supplementary material

Crystallographic data in this article have been deposited with the Cambridge Crystallographic Data Centre as supplementary publication No. CCDC–825719 for **1**. Copies of the data can be obtained free of charge on application to CCDC, 12 Union Road, Cambridge CB2 1EZ, UK (Tel: +44 (0) 1223 762-911 or E-mail: deposit@ccdc.cam.ac.uk).

Acknowledgments

The support from the Key Laboratory of Environmental Engineering, Protection and Assessment of Guangxi, the National Water Pollution Control and Management of China (No. 2008ZX07317–02) are greatly appreciated.

References

[1] M. Gielen. *Appl. Organomet. Chem.*, **16**, 481 (2002).
[2] E.R.T. Tiekink. *Trends Organomet. Chem.*, **1**, 71 (1994).
[3] S.L. Chen, Z. Liu, J. Liu, G.C. Han, Y.H. Li. *J. Mol. Struct.*, **1014**, 110 (2012).
[4] S. Bureekaew, S. Shimornura, S. Kitagawa. *Sci. Technol. Adv. Mater.*, **9**, 1 (2008).
[5] X.Y. Xu, R.S. Zhou, J.F. Song, J.Q. Xu. *Chem. Res. Chin. Univ.*, **25**, 279 (2009).
[6] W.G. Lu, L. Jiang, X.L. Feng, T.B. Lu. *Inorg. Chem.*, **48**, 6997 (2008).
[7] M.H. Alkordi, Y.L. Liu, R.W. Larsen, J.F. Eubank, M. Eddaoudi. *J. Am. Chem. Soc.*, **130**, 12639 (2008).
[8] R.C. Maurya, R. Verma, T. Singh. *Synth. React. Inorg. Met. Org. Chem.*, **33**, 309 (2003).
[9] I. Sheikhshoaei. *J. Coord. Chem.*, **56**, 463 (2003).
[10] C. Celik, M. Tümer, S. Serin. *Synth. React. Inorg. Met. Org. Chem.*, **32**, 1839 (2002).
[11] R. Ramesh, M. Sivagamasundari. *Synth. React. Inorg. Met. Org. Chem.*, **33**, 899 (2003).
[12] J. Lewinski, J. Zachara, I. Justyniak, M. Dranka. *Coord. Chem. Rev.*, **249**, 1185 (2005).
[13] H.J. Chen, J. Zhang, W.L. Feng, M. Fu. *Inorg. Chem. Commun.*, **9**, 300 (2006).
[14] X.J. Wang, M.X. Jiang, C.H. Zhan, Y.L. Feng, Y.H. He. *Chin. J. Struct. Chem.*, **30**, 31 (2011).
[15] J.J. Zhang, T.L. Sheng, S.Q. Xia, G. Leibeling, F. Meyer, S.M. Hu, R.B. Fu, S.C. Xiang, X.T. Wu. *Inorg. Chem.*, **43**, 5472 (2004).
[16] J.J. Zhang, S.M. Hu, L.M. Zheng, X.T. Wu, Z.Y. Fu, J.C. Dai, W.X. Du, H.H. Zhang, R.Q. Sun. *Chem. Eur. J.*, **8**, 5742 (2002).
[17] G. Férey. *Angew. Chem. Int. Ed.*, **42**, 2576 (2003).
[18] W.S. Wu, S.X. Liu, T.T. Huang, X.R. Lan. *Acta Chim. Sin.*, **61**, 1014 (2003).
[19] G.M. Sheldrick. *Acta Crystallogr. A*, **64**, 112 (2008).
[20] X.M. Li, Y.L. Niu, B. Liu, Q.W. Wang. *Chin. J. Inorg. Chem.*, **26**, 1319 (2010).
[21] G.C. Vlahopoulou, D.I. Alexandropoulos, C.P. Raptopoulou, S.P. Perlepes, A. Escuer, T.C. Stamatatos. *Polyhedron*, **28**, 3235 (2009).
[22] H.W. Liu, W.G. Lu. *Chin. J. Inorg. Chem.*, **26**, 529 (2010).
[23] Z.Q. Shi, N.N. Ji, X. Zhao, Z.B. Zheng. *Chin. J. Inorg. Chem.*, **26**, 251 (2010).
[24] C.Q. Wan, X. Li, C.Y. Wang, X. Qiu. *J. Mol. Struct.*, **930**, 32 (2009).
[25] J.M. Ugalde, I. Alkorta, J. Elguero. *Angew. Chem. Int. Ed.*, **39**, 717 (2000).
[26] A.L. Gillon, N. Feeder, R.J. Davey, R. Storey. *Cryst. Growth Des.*, **3**, 663 (2003).
[27] J.N. Moorthy, R. Natarajan, P. Venugopalan. *Angew. Chem. Int. Ed.*, **41**, 3417 (2002).
[28] S.H. Zhang, M.H. Zeng, H. Liang. *Chin. J. Struct. Chem.*, **27**, 785 (2008).
[29] X.M. Chen, S.H. Zhang, H.H. Zou, A.Z. Tan. *J. Coord. Chem.*, **61**, 2563 (2008).
[30] S.M. Anikumari, V. Shivaiah, S.K. Das. *Inorg. Chem.*, **41**, 6953 (2002).
[31] H.J. Hao, D. Sun, F.J. Liu, R.B. Huang, L.S. Zheng. *Cryst. Growth Des.*, **11**, 5475 (2011).
[32] Z.P. Li, L. Huang, P.X. Xi, H.Y. Liu, Y.J. Shi, G.Q. Xie, M. Xu, F.J. Chen, Z.Z. Zeng. *J. Coord. Chem.*, **64**, 1885 (2011).
[33] S.H. Zhang, Y.G. Wang, C. Feng, G.Z. Li. *J. Coord. Chem.*, **63**, 3697 (2010).
[34] L.X. Jin, S.H. Zhang, Z. Liu, G.Z. Li. *Acta Crystallogr.*, **E63**, m2631 (2007).
[35] L.E. Cheruzel, M.S. Pometun, M.R. Cecil, M.S. Mashuta, R.J. Wittebort, R.M. Buchanan. *Angew. Chem. Int. Ed.*, **42**, 5452 (2003).
[36] C.F. Yan, Q.H. Chen, L. Chen, R. Feng, X.C. Shan, F.L. Jiang, M.C. Hong. *Aust. J. Chem.*, **64**, 104 (2011).
[37] G.G. Luo, H.B. Xiong, J.C. Dai. *Cryst. Growth Des.*, **11**, 507 (2011).
[38] Z. Yang, S.G. Hua, W.J. Hua, S.H. Li. *J. Phys. Chem. B*, **115**, 8249 (2011).
[39] S.P. Chen, Y.X. Yuan, L.L. Pan, L.J. Yuan. *J. Inorg. Organonmet. Polym.*, **18**, 384 (2008).
[40] K. Raghuraman, K.K. Katti, L.J. Barbour, N. Pillarsetty, C.L. Barnes, K.V. Katti. *J. Am. Chem. Soc.*, **125**, 6955 (2003).
[41] C. Janiak, T.G. Scharmann. *J. Am. Chem. Soc.*, **124**, 14010 (2002).
[42] J.P. Zhang, Y.Y. Lin, X.C. Huang, X.M. Chen. *Inorg. Chem.*, **44**, 3146 (2005).
[43] R. Ludwig. *Angew. Chem. Int. Ed.*, **40**, 1808 (2001).

[44] X.M. Li, Y.C. Cui, Q.W. Wang, C.B. Li, R.Z. Wang, G.G. Gao. *Chin. J. Struct. Chem.*, **25**, 481 (2006).
[45] J.G. Yang, F.Y. Pan, J.M. Li. *Chin. J. Inorg. Chem.*, **21**, 1593 (2005).
[46] E. Szlyk, S. Surdykowski, M. Barwiolek, E. Larsen. *Polyhedron*, **21**, 2711 (2002).
[47] J.G. Yang, F.Y. Pan, W.P. Jia, F. Li. *Chin. J. Inorg. Chem.*, **25**, 2207 (2009).
[48] H.Y. Wang, P.S. Zhao, D.L. Shao, J. Zhang, Y.L. Zhu. *Struct. Chem.*, **20**, 995 (2009).
[49] P.B. Sreeja, M.R.P. Kurup, A. Kishare, C. Jasmin. *Polyhedron*, **23**, 575 (2003).
[50] R. Gup, B. Kırkan. *Spectrochim. Acta A*, **62**, 1188 (2005).
[51] B.Y.K. Ho, J.J. Zuckerman. *J. Inorg. Chem.*, **12**, 1552 (1973).
[52] A.M. Sakho, D.F. Du, W.J. Li, S.S. Liu, D.S. Zhu, L. Xu. *J. Coord. Chem.*, **63**, 2317 (2010).
[53] X.L. Hu, P.F. Shi, X.Y. Xu, D.Q. Wang, B.Y. Zhu. *Chin. J. Inorg. Chem.*, **24**, 241 (2008).
[54] S.K. Ghosh, P.K. Bharadwaj. *Inorg. Chem.*, **43**, 6887 (2004).
[55] S.K. Ghosh, P.K. Bharadwaj. *Eur. J. Inorg. Chem.*, 4886 (2005).
[56] S.K. Ghosh, P.K. Bharadwaj. *Eur. J. Inorg. Chem.*, 4880 (2005).
[57] Y. Jin, Y.X. Che, J.M. Zheng. *Inorg. Chem. Commun.*, **10**, 514 (2007).
[58] P.X. Xi, Z.H. Xu, F.J. Chen, Z.Z. Zeng, X.W. Zhang. *J. Inorg. Biochem.*, **103**, 210 (2009).
[59] R.X. Li, Y.Y. Deng, B.C. Liu, F.Q. Liu, Q.Y. Wu. *Chin. J. Inorg. Chem.*, **26**, 609 (2010).
[60] K. Jeyasubramanian, S.A. Ssamath, S. Thambidurai, R. Murugesan, S.K. Ramalingam. *Trans. Met. Chem.*, **20**, 76 (1995).